Section 1

Theoretical aspects of hydrologic optics

Limnol. Oceanogr., 34(8), 1989, 1389–1409

Can the Lambert-Beer law be applied to the diffuse attenuation coefficient of ocean water?

Howard R. Gordon
Department of Physics, University of Miami, Coral Gables, Florida 33124

Abstract

Radiative transfer theory is combined with a bio-optical model of Case 1 waters and an optical model of the atmosphere to simulate the transport of radiation in the ocean-atmosphere system. The results are treated as experimental data to study the downwelling irradiance attenuation coefficient. It is shown that the downwelling irradiance attenuation coefficient just beneath the surface and the mean downwelling irradiance attenuation coefficient from the surface to the depth where the irradiance falls to 10% of its value at the surface can be corrected for the geometric structure of the in-water light field to yield quantities that are—to a high degree of accuracy—inherent optical properties. For Case 1 waters these geometry-corrected attenuation coefficients are shown to satisfy the Lambert-Beer law with a *maximum* error of 5–10% depending on wavelength. This near-validity of the Lambert-Beer law, when there are compelling reasons to believe that it should fail, is shown to result from three *independent* facts: the dependence of the diffuse attenuation coefficients on the geometric structure of the light field can be removed; pure seawater is a much better absorber than scatterer at optical frequencies; and the phase function for particles suspended in the ocean differs significantly from that of pure seawater. Finally, it is shown that extrapolation of the corrected diffuse attenuation coefficients to the limit $c \rightarrow c_w$ yields quantities that are within 2% of the corresponding quantities that would be measured for an ocean consisting of pure seawater with the sun at zenith and the atmosphere removed.

In a series of papers, Smith and Baker (Baker and Smith 1982, and references therein) have developed a "bio-optical" model for relating the optical properties of near-surface ocean water to the content of biological material. Specifically, the attenuation coefficient K_d of downwelling irradiance E_d defined by $K_d = -(1/E_d)\, dE_d/dz$, where z is depth, is related to the phytoplankton pigment concentration C through

$$K_d = K_w + K_C(C) + K_x. \qquad (1)$$

C is the concentration of Chl a and all chlorophyll-like pigments that absorb in the same spectral bands as Chl a, such as pheophytin a, and are contained in phytoplankton or in their detrital material. In Eq. 1, the Lambert-Beer law applied to K_d, K_w is the contribution to K_d from the water itself, K_x is the contribution from material suspended or dissolved in the water and not covarying with C, and $K_C(C)$ represents the contribution to K_d from phytoplankton and their immediate detrital material (units given in list of symbols). This decomposition of K_d is very useful for the optical analysis of ocean water because of the relative ease in measuring E_d, the absence of the requirement for absolute radiometry to determine K_d, and the possibility of measuring K_d remotely (Austin and Petzold 1981; Gordon 1982) and even at night (Gordon 1987). To utilize it, we plot measurements of K_d for a given wavelength and from a variety of oceanic waters as a function of C and assume the minimum envelope of the resulting curve, $(K_d)_{\min}$, corresponds to $K_x = 0$.

Acknowledgments

This work received support from the Office of Naval Research under contract N00014-84-K-0451 and grant N00014-89-J-1985, and from the National Aeronautics and Space Administration under grant NAGW-273.

Taking the limit of $(K_d)_{\min}$ as $C \rightarrow 0$ yields K_w. Then, $K_C(C)$ is given by $(K_d)_{\min} - K_w$. (For an example of this procedure *see* figure 1 of Baker and Smith 1982.) If we assume that $K_C(C)$ is valid for all waters, Eq. 1 can be applied to specific cases to estimate K_x from K_d and C or to estimate C from K_d in waters for which K_x is known to be negligible. These latter waters are usually referred to as "Case 1 waters" and are defined to be waters for which the optical properties are controlled by phytoplankton and their immediate detrital material (Gordon and Morel 1983; Morel and Prieur 1977). Limiting the analysis to Case 1 waters, Gordon and Morel (1983) and Morel (1988) used Eq. 1 to derive $K_C(C)$ by assuming $K_x = 0$.

Equation 1 has been criticized by Morel and Bricaud (1981) and Stavn (1988) on the basis that, unlike the absorption coefficient and the volume scattering function, K_d is not solely a property of the medium. This is because it depends on the depth (even for a homogeneous ocean) and on the geometric structure of the light field incident on the sea surface, as well as on the properties of the medium. Since a given K_d is unique only to the particular situation in which it is measured, and there is no reason to expect that the three components of K_d will vary in the same manner with depth and with the structure of the incident light field, it is correctly asserted that Eq. 1 can only be an approximation. However, Gordon et al. (1975) have shown with Monte Carlo simulations of the in-water light field that for simple modes of illumination (i.e. a sky of uniform radiance or a parallel beam of irradiance incident at an angle ϑ_0 with the vertical), the dependence of K_d on the structure of the incident light field can be removed without any knowledge of the optical properties of the medium. Gordon (1976) showed that the correction factor required to remove the light field dependence from K_d could be computed with reasonable accuracy by knowing only the relative amounts of skylight and direct sunlight incident on the sea surface in the spectral band in question. Later, Baker and Smith (1979) directly verified that for turbid water under clear skies, K_d was nearly independent of ϑ_0 for $\vartheta_0 \lesssim 40°$. Finally, Gordon (1980) demonstrated that for a stratified ocean with sun at zenith the value of K_d at a given depth depended mostly on the properties of the medium *at that depth*, i.e. K_d is a *local* property of the medium. These observations suggest that if K_d values were corrected for variations in illumination (e.g. corrected so that they are referenced to a standard incident illumination) and used in Eq. 1, the error resulting from the fact that K_d is not a true property of the medium would be considerably reduced. But a residual error would remain in Eq. 1 because K_d depends on depth.

In this paper the earlier computations (Gordon et al. 1975) of K_d are extended to cases of more realistic illumination of the surface and a realistic model of the optical properties of the ocean. It begins with a review of the equation which governs the transport of radiant energy in the ocean and in the atmosphere, and of the basic optical properties (e.g. absorption and scattering coefficients, etc.) required to obtain a solution. A realistic model of these optical properties is then presented and the results of Monte Carlo simulations of the in-water light field are used to study the properties of K_d. The analysis of K_d shows that when it is measured either just beneath the surface, or when an average value is determined between the surface and the depth where the surface irradiance is reduced to 10% of its value at the surface, the resulting K_d can be corrected to yield a quantity that can be directly expressed in terms of the optical properties of the medium. Furthermore, the corrected K_d values are shown to depend almost linearly on the optical properties of the medium, which in turn are linearly additive over the constituents, and so the corrected values will satisfy the Lambert-Beer law with reasonable accuracy. Finally, the computations show that the value of K_w determined by extrapolation of K_d to $C = 0$ in Case 1 waters is very nearly equal to the value of K_d that would be measured in an ocean consisting of only pure seawater.

The radiative transfer equation and optical properties

Consider an ocean in which the optical properties and sources depend only on the depth z. The steady state light field in the

Significant symbols

a	Total absorption coefficient, m^{-1}	K	$K_d(0)$, m^{-1}
a_p	Particle absorption coefficient, m^{-1}	K^I	Inherent value of $K_d(0)$, m^{-1}
a_w	Water absorption coefficient, m^{-1}	K_w	Pure water component of $K_d(0)$ and $K_d(z)$, m^{-1}
b	Total scattering coefficient, m^{-1}		
b_b	Total backscattering coefficient, m^{-1}	K_p	Particle component of K, m^{-1}
$\tilde{b}_b$	Total backscattering probability	K_C	Pigment component of $K_d(z)$, m^{-1}
b_p	Particle scattering coefficient, m^{-1}	K_x	Nonpigment-nonwater component of $K_d(z)$, m^{-1}
b_w	Water scattering coefficient, m^{-1}		
$\beta(\Theta)$	Total volume scattering function, m^{-1} sr^{-1}	$\langle K \rangle$	Mean $K_d(z)$ from surface to z_{10}, m^{-1}
		$\langle K \rangle^I$	Inherent value of $\langle K \rangle$, m^{-1}
$\beta_p(\Theta)$	Particle volume scattering function, m^{-1} sr^{-1}	$\langle K \rangle_w$	Water component of $\langle K \rangle$, m^{-1}
		$\langle K \rangle_w^I$	Inherent value of $\langle K \rangle_w$, m^{-1}
$\beta_w(\Theta)$	Water volume scattering function, m^{-1} sr^{-1}	$\langle K \rangle_p$	Particle component of $\langle K \rangle$, m^{-1}
		$\langle K \rangle_B$	Lambert-Beer value of $\langle K \rangle$ ($\langle K \rangle_w + \langle K \rangle_p$), m^{-1}
$\beta_i^*(\Theta)$	Specific volume scattering function (β_i / C_i), m^2 mg^{-1} sr^{-1}		
		$\langle K \rangle_T$	True value of $\langle K \rangle$, m^{-1}
c	Total attenuation coefficient ($a + b$), m^{-1}	$K_u(z)$	Attenuation coefficient for $E_u(z)$, m^{-1}
c_p	Particle attenuation coefficient ($a_p + b_p$), m^{-1}	$L(z; \vartheta, \varphi)$	Radiance traveling in direction (ϑ, φ), mW $(cm^2\ \mu m\ sr)^{-1}$
c_w	Water attenuation coefficient ($a_w + b_w$), m^{-1}	λ	Wavelength, nm
		$\bar{\mu}$	Average cosine of $L(z; \vartheta, \varphi)$
c_i	Attenuation coefficient of component i, m^{-1}	$\bar{\mu}_w$	Average cosine when $c_p = 0$
		$\bar{\mu}_p$	Average cosine when $c_w = 0$
c_i^*	Specific attenuation coefficient c_i/C_i, m^2 mg^{-1}	$P(\Theta)$	Scattering phase function (β/b), sr^{-1}
		$P_p(\Theta)$	Particle scattering phase function (β_p/b_p), sr^{-1}
C	Pigment concentration, mg m^{-3}		
C_i	Concentration of ith constituent, mg m^{-3}	$P_w(\Theta)$	Water scattering phase function (β_w/b_w), sr^{-1}
D_0	Downwelling distribution function ($\omega_0 = 0$)	$Q(z; \vartheta, \varphi)$	Intensity density of internal sources, mW $(cm^3\ \mu m\ sr)^{-1}$
f	Direct sun fraction of $E_d(0)$		
F	Total forward scattering probability ($1 - \tilde{b}_b$)	σ^2	Surface slope variance
		t	Fresnel transmittance of sea surface
F_p	Particle forward scattering probability	τ	Optical depth ($\tau = cz$)
F_w	Water forward scattering probability	τ_{10}	Optical depth at 10% surface irradiance (cz_{10})
F_0	Extraterrestrial solar irradiance, mW cm^{-2} μm^{-1}	τ_A	Aerosol optical thickness of atmosphere
		τ_{Oz}	Ozone optical thickness of atmosphere
$E_d(z)$	Downwelling irradiance at z, mW cm^{-2} μm^{-1}	τ_R	Rayleigh optical thickness of atmosphere
		(ϑ, φ)	Direction of radiant energy flow
E_d(sun)	Direct sun component of surface irradiance, mW cm^{-2} μm^{-1}	Θ	Scattering angle
		ϑ_0	Solar zenith angle
E_d(sky)	Sky component of surface irradiance, mW cm^{-2} μm^{-1}	ϑ_{0w}	Solar zenith angle below surface
		ω_0	Total scattering albedo (b/c)
$E_u(z)$	Upwelling irradiance at z, mW cm^{-2} μm^{-1}	ω_p	Particle scattering albedo (b_p/c_p)
		ω_w	Water scattering albedo (b_w/c_w)
$E_0(z)$	Scalar irradiance at z, mW cm^{-2} μm^{-1}	Ω	Solid angle, sr
$E_{0d}(z)$	Downwelling scalar irradiance at z, mW cm^{-2} μm^{-1}	z	Depth, m
		z_{10}	Depth at 10% surface irradiance, m
$K_d(z)$	Attenuation coefficient for $E_d(z)$, m^{-1}	z_x, z_y	Surface slope components
$K_d^I(z)$	Inherent value of $K_d(z)$ at z, m^{-1}		

ocean is described by the radiant power per unit area per unit solid angle called the radiance $L(z; \vartheta, \varphi)$, where ϑ and φ are the polar and azimuth angles (in a spherical coordinate system in which the z-axis is into the ocean and the x- and y-axes are along the ocean surface) of a vector in the direction the radiant energy is flowing. The distribution of radiance in the ocean is governed by the radiative transfer equation (RTE):

$$\cos\vartheta \frac{dL(z; \vartheta, \varphi)}{dz} = -c(z)L(z; \vartheta, \varphi) + \int_{\Omega'} \beta(z; \vartheta', \varphi' \to \vartheta, \varphi) \cdot L(z; \vartheta', \varphi')\, d\Omega' + Q(z; \vartheta, \varphi)$$

where $c(z)$ is the beam attenuation coefficient, $\beta(z; \vartheta', \varphi' \rightarrow \vartheta, \varphi)$ the volume scattering function for the scattering of radiance from a direction specified by (ϑ', φ') to that specified by (ϑ, φ), and $d\Omega'$ a differential element of solid angle around the direction (ϑ', φ'). The subscript Ω' on the integral indicates that the integration is to be taken over the entire range of $d\Omega'$ (i.e. 4π sr). The last term, $Q(z; \vartheta, \varphi)$ is the intensity density (radiant power per unit volume per unit solid angle) of internal sources *in* the ocean such as fluorescence (Gordon 1979), Raman scattering (Stavn and Weidemann 1988), bioluminescence (Gordon 1987), etc.

The total scattering coefficient $b(z)$ is related to the volume scattering function through

$$b(z) = \int_{\Omega'} \beta(z; \vartheta', \varphi' \rightarrow \vartheta, \varphi)\, d\Omega' = 2\pi \int_0^{\pi} \beta(z; \Theta) \sin \Theta\, d\Theta,$$

where Θ is the angle between the directions specified by (ϑ', φ') and (ϑ, φ). The beam attenuation coefficient is given by

$$c(z) = a(z) + b(z)$$

where $a(z)$ is the absorption coefficient of the medium. The radiance, a, b, c, β, and Q all depend on the wavelength λ of the light; however, this dependence has not been explicitly shown in these equations. It has been shown (Case 1957) that given the radiance incident on the sea surface [$L(0; \vartheta, \varphi)$ for $\vartheta < \pi/2$] and the sources within the ocean, the RTE has unique solutions if $b(z)/c(z) < 1$, i.e. in an ocean that has *some* absorption throughout. The RTE also applies to the combined ocean-atmosphere system when $z = 0$ is taken to be the top of the atmosphere; however, in this case L must be replaced by $L\, m^{-2}$, where m is the index of refraction of the medium ($m \approx 1$ for the atmosphere and ≈ 1.33 for the ocean). Also, Snell's law, the law of reflection, and the Fresnel equations must be used to propagate the radiance across the air–water interface. The incident radiance on the boundary of the ocean-atmosphere system is simply a beam of parallel light from the sun: $L(0; \vartheta, \varphi) = L_s \delta(\vartheta - \vartheta_0)\delta(\vartheta - \varphi_0)$, where L_s is the average radiance of the solar disk, (ϑ_0, φ_0) the direction with which the solar beam enters the top of the atmosphere, and δ the Dirac delta function.

The quantities $a(z)$, $b(z)$, $c(z)$, and $\beta(z; \Theta)$ depend only on the constituents of the medium and are known as the *inherent* optical properties (IOPs) (Preisendorfer 1976). Note that only two of these, a and β, are required to specify the full set. They are all linearly additive over the constituents, i.e. if β_w is the volume scattering function of pure seawater and β_i that of the ith constituent,

$$\beta(\Theta) = \beta_w(\Theta) + \sum_i \beta_i(\Theta).$$

The individual IOPs are directly proportional to the concentration of the constituents. For example, β_i is directly proportional to the concentration of ith constituent C_i:

$$\beta_i(\Theta) = \beta_i^*(\Theta)\, C_i$$

where β_i^* is called the *specific* volume scattering function. It is convenient to define two new IOPs: the scattering phase function,

$$P(z; \vartheta', \varphi' \rightarrow \vartheta, \varphi) \equiv \frac{\beta(z; \vartheta', \varphi' \rightarrow \vartheta, \varphi)}{b(z)},$$

and the single scattering albedo $\omega_0(z) \equiv b(z)/c(z)$. The RTE then becomes

$$\cos \vartheta \frac{dL(z; \vartheta, \varphi)}{c(z)\, dz} = -L(z; \vartheta, \varphi) + \omega_0(z) \cdot \int_{\Omega'} P(z; \vartheta', \varphi' \rightarrow \vartheta, \varphi) \cdot L(z; \vartheta', \varphi')\, d\Omega' + Q(z; \vartheta, \varphi)/c(z),$$

from which it is seen that there are no internal sources ($Q = 0$). When the true depth is scaled by the beam attenuation coefficient to form the optical depth τ, where $d\tau = c(z)\, dz$, the propagation of the radiance is determined only by $\omega_0(\tau)$ and the scattering phase function, i.e.

$$\cos \vartheta \frac{dL(\tau; \vartheta, \varphi)}{d\tau} = -L(\tau; \vartheta, \varphi) + \omega_0(\tau) \cdot \int_{\Omega'} P(\tau; \vartheta', \varphi' \rightarrow \vartheta, \varphi) \cdot L(\tau; \vartheta', \varphi')\, d\Omega'. \quad (2)$$

Radiance in the ocean is difficult to measure because of its dependence on ϑ and φ. Thus, most measurements of the oceanic light field are limited to integrals of the radiance. Three integrals particularly useful in marine optics are the downwelling E_d, upwelling E_u, and scalar E_0 irradiances defined by

$$E_d(z) = \int_0^{2\pi} d\varphi \int_0^{\pi/2} L(z; \vartheta, \varphi)\cos\vartheta \sin\vartheta \, d\vartheta,$$

$$E_u(z) = -\int_0^{2\pi} d\varphi \int_{\pi/2}^{\pi} L(z; \vartheta, \varphi)\cos\vartheta \sin\vartheta \, d\vartheta,$$

and

$$E_0(z) = \int_0^{2\pi} d\varphi \int_0^{\pi} L(z; \vartheta, \varphi)\sin\vartheta \, d\vartheta.$$

The irradiances E_d and E_u are the downward and upward flux (radiant power per unit area) of radiant energy across a horizontal surface at depth z. The scalar irradiance is proportional to the energy density of the light field at z. If the RTE (with $Q = 0$) is multiplied by $d\Omega$ and integrated over all Ω the result is Gershun's equation (Gershun 1939; Preisendorfer 1961):

$$\frac{d}{dz}[E_d(z) - E_u(z)] = -a(z)E_0(z).$$

The combination $E_d - E_u$ is called the vector irradiance and given the symbol $E(z)$. A quantity which will be of interest later is the "average cosine" $\bar{\mu}$ of the light field:

$$\bar{\mu}(z) = \frac{E(z)}{E_0(z)}.$$

From the definitions of E and E_0 it is seen that $\bar{\mu}$ is the average value of $\cos\vartheta$ weighted by the radiance distribution.

Of the three irradiances defined above, E_d has most often been measured and we center our interest on it. Observations in the ocean show that $E_d(z)$ (along with E_u and E_0) decreases approximately exponentially with depth, so it is useful to determine the exponential decay coefficient of E_d:

$$K_d(z) = -\frac{d\{\ln[E_d(z)]\}}{dz}$$

or

$$\frac{K_d(\tau)}{c} = -\frac{d\{\ln[E_d(\tau)]\}}{d\tau}.$$

K_d is the downwelling irradiance attenuation coefficient. For a homogeneous ocean (IOPs independent of z), it is a slowly varying function of depth (e.g. *see Fig. 3A*) and thus for a given distribution of radiance on the sea surface it could almost be considered a property of the medium; however, it also depends on the geometric structure of the light field (the radiance) in the water which in turn depends on the distribution of radiance incident on the sea surface (e.g. *see Fig. 3B*). If the latter is changed, the value of K_d will also change. Thus, in contrast to the IOPs, Preisendorfer (1976) has called K_d an apparent optical property (AOP) of the medium. Although he was able to relate $K_d(z)$ to the diffuse absorption and backscattering coefficients (which he called *hybrid* optical properties) exactly, these coefficients are not independent of the light field. In an analysis of this relationship, Kirk (1981, 1983) has shown that the diffuse backscattering coefficients bear little resemblance to their inherent counterpart, the true backscattering coefficient b_b given by

$$b_b = 2\pi \int_{\pi/2}^{\pi} \beta(\Theta)\sin\Theta \, d\Theta.$$

Thus, a direct relationship between K_d and the IOPs has yet to be established, and this is one of the bases for criticism of the application of the Lambert-Beer law to $K_d(z)$.

Optical model of the ocean-atmosphere system

The present study of the efficacy of Eq. 1 is based on solving the RTE in the ocean-atmosphere to determine $E_d(z)$ from which $K_d(z)$ is computed. To accomplish this requires realistic models of the IOPs of the ocean and the atmosphere. Such models are described below.

The ocean—As discussed earlier, water

and its constituents influence the in-water light field through their effect on a and β. For simplicity, we limit the modeling of these properties to Case 1 waters. Moreover, we also limit the model to those waters for which absorbing dissolved organic materials—yellow substances—are absent. The rationale for this is that the effect of yellow substance absorption on the results would be identical to that of increasing the absorption coefficient of pure seawater by an appropriate amount. Also, the medium is assumed to be homogeneous. Thus, the medium is described by an absorption coefficient, $a = a_w + a_p$, where the subscripts w and p here (and hereafter) refer to the contribution from water and suspended particles and a volume scattering function given by $\beta(\Theta) = \beta_w(\Theta) + \beta_p(\Theta)$. The total scattering coefficient b found by integrating β over solid angle is $b = b_w + b_p$. Likewise, the beam attenuation coefficient is given by $c = c_w + c_p = a + b$.

From the partial IOPs (i.e. a_w, a_p, β_w, and β_p), the parameters $P(\Theta)$ and ω_0 that are required in Eq. 2 for the ocean can be related to the similar water and particle quantities $P_w(\Theta)$, $P_p(\Theta)$, ω_w, and ω_p through

$$\omega_0 = \frac{\omega_p(c_p/c_w) + \omega_w}{c_p/c_w + 1}, \tag{3}$$

and

$$\omega_0 P = \frac{\omega_p P_p(c_p/c_w) + \omega_w P_w}{c_p/c_w + 1}. \tag{4}$$

Thus, in this model, given ω_w, ω_p, $P_w(\Theta)$, and $P_p(\Theta)$, representing the inherent optical properties of the water and of the particles, ω_0 and $P(\Theta)$ are specified by the ratio c_p/c_w. This ratio is proportional to the particle concentration.

Experimental measurements must be used to provide a realistic parameterization of the IOPs ω_w, ω_p, $P_w(\Theta)$, and $P_p(\Theta)$. These IOPs are functions of the wavelength λ of the light, and therefore, in what follows, the wavelength will be explicitly displayed in the equations, e.g. $b_p(\lambda)$ refers to the scattering coefficient at the wavelength λ. The model used here is identical to the one I developed (Gordon 1987) to study the propagation of irradiance from a point-source embedded in the ocean. Briefly, the absorption coefficient a_w has been inferred from measurements of downwelling and upwelling irradiance in oligotrophic waters such as the Sargasso Sea (Morel and Prieur 1977; Prieur and Sathyendranath 1981; Smith and Baker 1981), and the scattering coefficient b_w and the volume scattering function $\beta_w(\Theta)$ have been measured directly for pure water and for saline solutions of pure water corresponding to salinities between 35 and 39‰ by Morel (1974). The resulting a_w, b_w, and ω_w are given in Table 1 for the wavelengths used in the present computations. Note that these values of ω_w represent the *upper limit* of the scattering albedo for water plus any *dissolved* material such as yellow substances, since dissolved material typically found in seawater can contribute to the absorption coefficient but not to the scattering coefficient. The scattering phase function for pure seawater is from Morel (1974).

The optical properties of the suspended particles for Case 1 waters can be related to pigment concentration. The scattering coefficient of particles at 550 nm, $b_p(550)$, is nonlinearly related to the pigment concentration C through (Morel 1980).

$$b_p = B_C C^{0.62} \tag{5}$$

where $b_p(550)$ is in m^{-1} and C is in mg m^{-3} (*see also* Gordon and Morel 1983). The constant B_C—the scattering coefficient at a pigment concentration of 1 mg m^{-3}—ranges from 0.12 to 0.45 and has an average value of 0.30. The variation in B_C is due to the natural variability of scattering over the various species of phytoplankton, as well as variability in scattering by detrital particles associated with the phytoplankton. Similarly the absorption coefficient of the particles has been studied as a function of C by Prieur and Sathyendranath (1981), yielding for $C < 10$ mg m^{-3}:

$$a_p(\lambda) = 0.06 A_C(\lambda) C^{0.602}, \tag{6}$$

where $a_p(\lambda)$ is in m^{-1} and C is in mg m^{-3}. In this equation $A_C(\lambda)$ is the absorption coefficient of phytoplankton normalized to 440 nm:

$$A_C(\lambda) = \frac{a_p(\lambda)}{a_p(440)}.$$

Table 1. Absorption and scattering coefficients of pure seawater.

λ (nm)	b_w (m^{-1})	a_w (m^{-1})	ω_w
440	0.0049	0.0145	0.253
480	0.0034	0.0176	0.162
550	0.0019	0.0638	0.029

Table 2. Model values of ω_p and ω_w.

λ (nm)	ω_p	ω_w
440	0.86	0.253
480	0.88	0.162
550	0.93	0.029

The relative absorption of phytoplankton $A_C(\lambda)$ deduced by Prieur and Sathyendranath (1981) agrees well with absorption measurements made on phytoplankton cultures by Sathyendranath (1981). Note that $a_p(\lambda)$ includes both phytoplankton and their detrital material and thus represents the absorption of all components other than the water itself. These nonlinear relationships between b_p and C and a_p and C are believed to be due to a systematic variation in the ratio of the concentration of phytoplankton to that of detrital material as a function of the concentration of phytoplankton (Hobson et al. 1973; Smith and Baker 1978*a*). Since $b_p(\lambda)$ and $a_p(\lambda)$ vary with pigment concentration in nearly the same manner, $b_p(\lambda)/a_p(\lambda)$ is nearly independent of the pigment concentration:

$$\frac{b_p(\lambda)}{a_p(\lambda)} \approx 16.6\frac{B_C(\lambda)}{A_C(\lambda)}.$$

This relation provides an estimate of $\omega_p(\lambda)$ and shows that this quantity is, in the first approximation, *independent* of pigment concentration. At 550 nm, where an average B_C is known, it yields $\omega_p(550) = 0.933$, in good agreement with the range for those measured by Bricaud et al. (1983) for four species of cultured phytoplankton: $0.89 \leq \omega_p(550) \leq 0.97$. To fix reasonable values of $\omega_p(\lambda)$ at the other wavelengths of interest, we require the variation of B_C with λ. Following Gordon (1987) we assume $B_C(\lambda)$ obeys a power law with wavelength (i.e.) $B_C(\lambda) \propto \lambda^{-n}$ and take $n = +1$. This yields $B_C(480) \approx 0.34$ and $B_C(440) \approx 0.38$. The resulting values of $\omega_p(\lambda)$ and $\omega_w(\lambda)$ used in the computations are provided in Table 2. It should be noted that the assumption $B_C(\lambda) \propto \lambda^{-1}$ often overestimates the dependence of b_c on λ since the scattering by absorbing particles (e.g. phytoplankton) tends to be *depressed* in the pigment absorption bands (Bricaud et al. 1983). This depression of scattering would make $\omega_p(440)$ and $\omega_p(480)$ smaller than given in Table 2; however, the effect is not large, e.g. changing n from $+1$ to -1 only reduces $\omega_p(440)$ from 0.86 to 0.80. To ensure that wide departures of ω_p from those used in Table 2 do not influence the results of this work, I have also carried out simulations for $\omega_p(480) = 0.5$, 0.7, and 0.99.

The particle phase function is the most difficult quantity to parameterize because it requires the individual phase functions of the plankton and the detrital material—neither of which have ever been measured in the field. Thus, we must rely on measurements of the total particle phase function (plankton plus detrital material). Measurements of the volume scattering function at 530 nm have been made for waters in several locations with very different turbidities (total scattering coefficients) by Petzold (1972). When the scattering by pure seawater is subtracted, the resulting particle phase functions are very similar, having a standard deviation within about 30% of the mean, over waters for which the particle scattering coefficient varied over a factor of 50. This mean particle phase function derived from Petzold's measurements is adopted for this study and designated by the symbol "M." Also, two other particle phase functions are used to represent the extremes of the phase functions given by Petzold's measurements: the mean of three phase functions measured in the turbid waters of San Diego Harbor and designated by "T," and a phase function measured in the clear waters of the Tongue of the Ocean, Bahamas, and designated by "C." The three particle phase functions are shown in Fig. 1 along with the phase function for scattering by the water itself [$P_w(\Theta)$]. We see that these model phase functions differ principally in their scattering at angles $>25°$.

This completes the specification of the

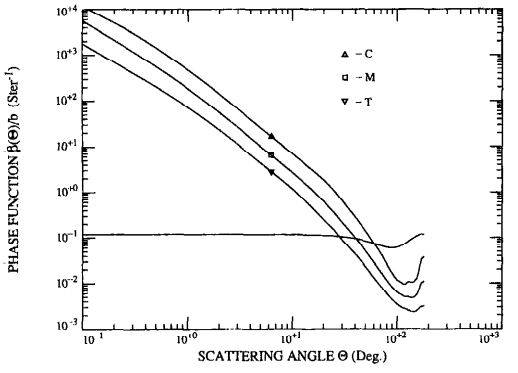

Fig. 1. Phase functions for particles and water. Phase functions M and C have been multiplied by 2 and 4, respectively, to facilitate plotting.

quantities needed for the simulation: ω_w, ω_p, $P_w(\Theta)$, and $P_p(\Theta)$. Varying the parameter c_p/c_w from 0 to ∞ results in models which range from a particle-free ocean to an ocean in which the optical properties of the particles are completely dominant. This parameter can be related to the pigment concentration through the bio-optical model by noting that $c_p = a_p + b_p$ and using Eq. 5 and 6. The result is

$$\frac{c_p(\lambda)}{c_w(\lambda)} \simeq \gamma(\lambda)C^{0.6}, \qquad (7)$$

where $\gamma(\lambda)$ = 22.4, 18.5, and 4.9 at 440, 480, and 550 nm.

The atmosphere—The atmosphere influences the in-water light field by distributing a portion of the near-parallel solar beam over the entire upward hemisphere (i.e. in producing sky light from direct sunlight). To simulate the angular distribution of radiation entering the ocean requires an atmospheric model. This model atmosphere consisted of 50 layers and included the effects of aerosols, ozone, and Rayleigh scattering, vertically distributed according to data taken from the work of Elterman (1968). The aerosol phase functions were computed by R. Fraser (pers. comm.) from Mie theory with the Deirmendjian (1969) Haze C size distribution. This model simulates optical properties of the cloud-free atmosphere only.

Computations and properties of K_d

With the above model for the IOPs of the ocean and atmosphere, the transport of radiant energy is *simulated* by Monte Carlo methods yielding the irradiance in the water. This is a numerical solution of Eq. 2 which fully accounts for multiple scattering in the ocean and in the atmosphere, including ocean-atmosphere coupling (i.e. light can scatter out of the ocean and then backscatter from the atmosphere and re-enter the ocean, etc.). In most of the simulations the sea surface is flat. As in all Monte Carlo simulations, the computed values of $E_d(z)$ contain statistical uncertainties. On the basis of the number of photons processed in each computer run, the maximum error (SD) in E_d just beneath the surface is less than $\pm 0.3\%$. This error increases with depth, reaching $\pm 1\%$ where E_d falls to 10% of its value at the surface and $\pm 3\%$ where E_d is 1% of its value at the surface.

To assess the errors in Eq. 1, we use the simulations to provide K_d as a function of C. Specifically, the various model oceans are generated by allowing the pigment concentration C to vary from 0 to about 4.5 mg m^{-3} which in turn causes c_p/c_w at each wavelength to vary according to Eq. 7. This variation in c_p/c_w then induces variations in ω_0 and $P(\Theta)$ determined by Eq. 3 and 4. Figure 2, for example, shows the change in the shape of the total phase function at 480 nm as c_p/c_w is varied from 0 to 100. Note how the phase function deviates strongly from that of pure water (Rayleigh scattering) even when $c_p/c_w = 1$, i.e. even when the total attenuation is shared equally between water and particles. To simulate a variety of cloud-free situations, I have carried out the computations for solar zenith angles of 0°, 20°, 25°, 30°, 40°, 60°, and 80°. Also, to simulate a totally overcast sky, I have studied each ocean model with the atmosphere removed and a totally diffuse light field incident on the sea surface. Thus, only situations with broken clouds are not considered here. A sky with broken clouds is particularly difficult to examine because the radiation field is no longer independent of the observer's horizontal position in the medium.

For the analysis, the resulting values of $E_d(z)$ from the simulations are treated as experimental data, albeit data collected under carefully controlled conditions—a cloud-free sky and a homogeneous ocean of *precisely known inherent optical properties*—

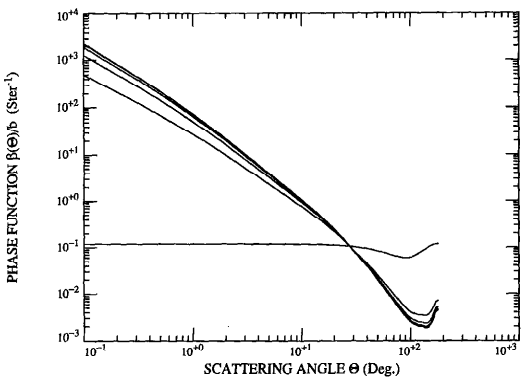

Fig. 2. Total phase function at 480 nm as a function of the particle concentration. Progressing from bottom to top on the left of the graph, c_p/c_w = 0, 1, 3, 10, and 100.

from which K_d can be determined by numerical differentiation and related to the IOPs of the ocean and ultimately to the constituent concentrations. Where comparison of the resulting K_d values with computations by Kirk (1984) is possible, i.e. K_d computed at the midpoint of the euphotic zone using particle phase function T with c_p/c_w very large and the atmosphere removed, the agreement is excellent.

Figure 3A provides some samples of the resulting profiles of the irradiance attenuation coefficient. In these examples K_d/c_w is computed for c_p/c_w = 0, 1.4, and 3.7 for particle phase function M at 440 nm with the sun at zenith. The deepest computed point for each profile corresponds to $\tau = 9$. These particular profiles represent a clear ocean (i.e. $C \leq 0.05$ mg m^{-3}) with c_p/c_w = 0 corresponding to pure seawater. The immediate conclusion to be drawn from these simulations is, as mentioned earlier, that K_d is dependent on depth even for a homogeneous ocean. Also, K_d near the surface increases more rapidly with z as c_p/c_w increases. In fact, from the surface to z = 100 m, K_d increases by 2.5, 10, and 20% for c_p/c_w = 0, 1.4, and 3.7, respectively. Figure 3B provides K_d/c_w at 440 nm as a function of depth with $c_p/c_w = 5.6$ ($C = 0.1$ mg m^{-3}) for three solar zenith angles (ϑ_0 = 0°, 20°, and

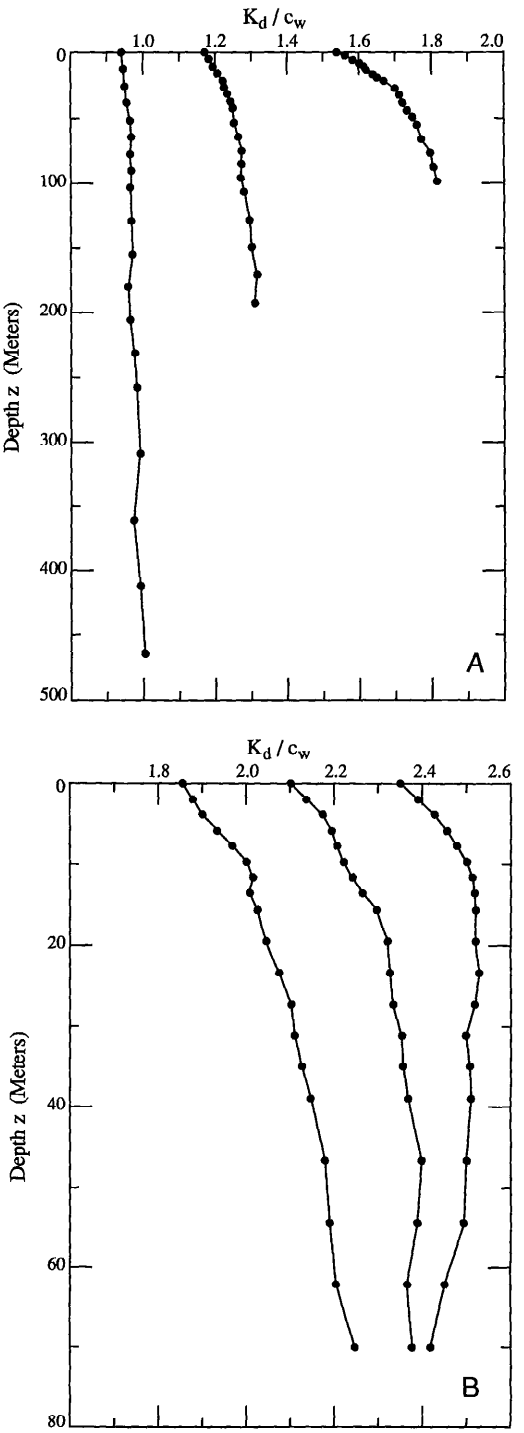

→

Fig. 3. A. Computed dependence of K_d/c_w on depth at 440 nm for particle phase function M. The three cases from left to right are for c_p/c_w = 0, 1.4, and 3.7. B. Computed dependence of K_d/c_w on depth at 440 nm for particle phase function M with $c_p/c_w = 5.6$. The three cases from left to right correspond to ϑ_0 = 0°, 20°, 40°.

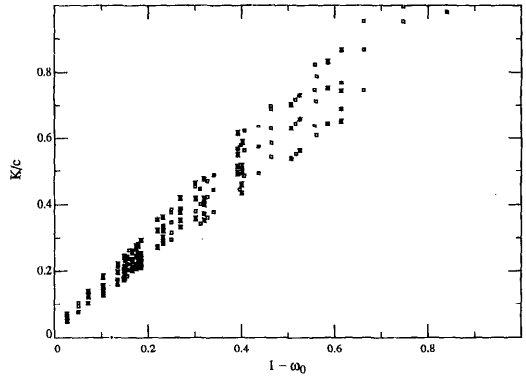

Fig. 4. K/c as a function of $1 - \omega_0$. The symbol code is given on Fig. 1. Note, $1 - \omega_0 = a/c$.

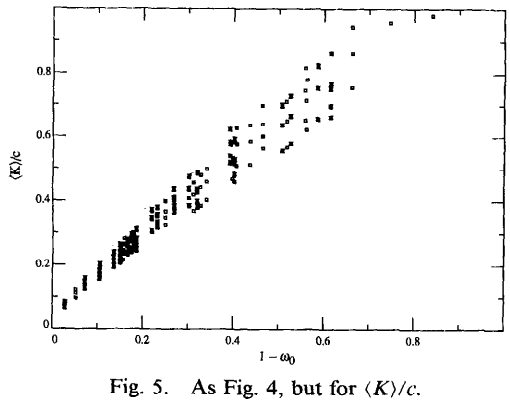

Fig. 5. As Fig. 4, but for $\langle K \rangle / c$.

40°). It shows that K_d in the upper 70 m is also strongly dependent on the incident radiance distribution as well as on depth.

These computations confirm the argument that K_d cannot be considered an inherent optical property because it depends on depth and on the incident radiance distribution. [An exception to this of course is the asymptotic light field ($z \to \infty$) for which it has been shown (Preisendorfer 1959) that K_d becomes independent of depth and independent of the incident radiance distribution. The asymptotic values of K_d/c_w for the examples in Fig. 3 are 1.00, 1.38, 1.95, and 2.42 for $c_p/c_w = 0$, 1.4, 3.7, and 5.6.] Thus, if we attempt to use K_d as an inherent optical property, it is necessary to specify in some manner the depth at which the measured value applies and to remove the dependence on the incident radiance distribution. Here we focus on the irradiance attenuation coefficient (K) just beneath the surface, i.e.

$$K = \lim_{\tau \to 0} K_d(\tau),$$

and on the average diffuse attenuation coefficient ($\langle K \rangle$) over the upper half of the euphotic zone,

$$\frac{\langle K \rangle}{c} = -\frac{\ln[E_d(\tau_{10})/E_d(0)]}{\tau_{10}}$$

where τ_{10} is the optical depth for which E_d falls to 10% of its value just beneath the surface [$E_d(\tau_{10})/E_d(0) = 0.1$]. Although difficult to measure because of wave-induced light-field fluctuations, K is valuable for showing the way toward a useful representation of K_d in terms of the IOPs. In contrast, $\langle K \rangle$ is relatively simple to measure. On the basis of the number of photons contributing to K and $\langle K \rangle$, the statistical uncertainty $\delta K/c$ in K/c is $\approx \pm 0.012$, while the *relative* error $\delta\langle K \rangle$ in $\langle K \rangle$ is about ± 0.006, i.e. $\delta\langle K \rangle / \langle K \rangle \approx \pm 0.006$.

Figures 4 and 5 provide the computations of K/c and $\langle K \rangle / c$ as a function of ω_0 for 334 simulations comprising various values of ϑ_0 and C for each particle phase function and wavelength. Note that $1 - \omega_0 = a/c$, so these figures relate K and $\langle K \rangle$ to the absorption coefficient a. Although a strong trend of increasing K/c and $\langle K \rangle / c$ with an increasing absorption component in the total attenuation is observed, it is clear (as expected) that the variation in K and $\langle K \rangle$ cannot be explained solely on the basis of the total absorption and scattering coefficients of the medium alone.

To proceed further it is useful to review the results of earlier investigations. Gordon et al. (1975) found that the dependence of $K_d(\tau)$ on the scattering phase function could be approximately removed by expressing $K_d(\tau)$ as a function of $\omega_0 F$, where F is the forward scattering probability ($F = 1 - \tilde{b}_b$, where $\tilde{b}_b = b_b/b$), rather than ω_0 alone. Also, they found that the effect of the nature of the illumination of the ocean on $K_d(\tau)$ could be understood by examining $K_d(\tau)/D_0(\tau)$, where $D_0(\tau)$ was the downwelling distribution function (Preisendorfer 1961) for a *to-*

Table 3. D_0 just beneath the sea surface.

ϑ_0	440 nm	480 nm	550 nm	$1/\cos \vartheta_{0w}$
0°	1.034	1.027	1.019	1.000
20°	1.074	1.065	1.055	1.035
25°	1.088	1.077	1.067	1.054
30°	1.105	1.100	1.093	1.079
40°	1.158	1.154	1.149	1.142
60°	1.286	1.293	1.299	1.315
80°	1.284	1.311	1.346	1.484
Diffuse	1.197	1.197	1.197	

tally absorbing ocean with the same surface illumination, i.e.

$$D_0(\tau) = \frac{E_{0d}(\tau)}{E_d(\tau)}$$

with $\omega_0 = 0$, where E_{0d} is the downwelling *scalar* irradiance defined by

$$E_{0d}(z) = \int_0^{2\pi} \mathrm{d}\varphi \int_0^{\pi/2} L(z; \vartheta, \varphi) \sin \vartheta \, \mathrm{d}\vartheta.$$

In the revised suggested notation (Morel and Smith 1982) for optical oceanography $D_0(\tau) = 1/\bar{\mu}_d$ for $\omega_0 = 0$, where $\bar{\mu}_d$ is the "average cosine" of the downwelling light field evaluated just beneath the surface. In the Gordon et al. (1975) study there was no atmosphere over the ocean, and in that case $D_0(\tau) = 1/\cos \vartheta_{0w}$, where ϑ_{0w} is the solar zenith angle measured *beneath* the sea surface. In the present simulations this is no longer valid because of the presence of the atmosphere, and D_0 is also dependent on wavelength because the amount of skylight produced by scattering in the atmosphere is a function of wavelength. Therefore, D_0 has been computed at each wavelength and for each solar zenith angle by directly solving the transfer equation for the given λ and ϑ_0 with $\omega_0 = 0$. The results of this computation for D_0 just beneath the surface ($\tau = 0$) are given in Table 3. The statistical errors in $E_d(0)$ and $E_{0d}(0)$ are $\pm 0.3\%$, so the error in $D_0(0)$ will normally be $\lesssim \pm 0.4\%$. Note that, as expected, D_0 usually increases with increasing ϑ_0; however, for 440 nm the contribution from the increasing amount of skylight compared to direct sunlight from $\vartheta_0 = 60°$ to $\vartheta_0 = 80°$ actually causes a small decrease in D_0. Also, for $\vartheta_0 \leq 60°$ the difference between $D_0(0)$ and $1/\cos \vartheta_{0w}$ is usually $\lesssim 3\%$. $D_0(\tau)$ also depends on τ; however, this dependence is of little interest here.

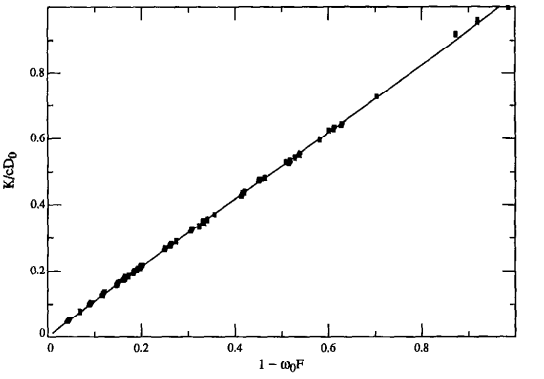

Fig. 6. K/cD_0 as a function of $1 - \omega_0 F$. The symbol code is given on Fig. 1.

Applying the observations from previous studies to the computations in Figs. 4 and 5, ω_0 is replaced by $\omega_0 F$ and K/c and $\langle K \rangle / c$ are replaced by K/cD_0 and $\langle K \rangle / cD_0$, where D_0 is the value of $D_0(0)$ taken from Table 3. This new scaling of the computations is presented in Figs. 6 and 7. We see that when the computations are presented in this manner, K/cD_0 and $\langle K \rangle / cD_0$ fall on what appear to be *universal* curves. The curves on the figures are least-squares fits of the points to

$$\frac{K}{cD_0} = \sum_{n=1}^{2} k_n (1 - \omega_0 F)^n, \qquad (8)$$

and

$$\frac{\langle K \rangle}{cD_0} = \sum_{n=1}^{3} \langle k \rangle_n (1 - \omega_0 F)^n, \qquad (9)$$

with $k_1 = 1.0617$, $k_2 = -0.0370$, $\langle k \rangle_1 = 1.3197$, $\langle k \rangle_2 = -0.7559$, and $\langle k \rangle_3 = 0.4655$. The average error in the least-squares fit to Eq. 8 and 9, is 1.8 and 2.2%. [Replacing $D_0(0)$ by $D_0(\tau_{10})$ in Eq. 9 provides no significant increase in the quality of the expansion.] Also, a linear fit of K/cD_0 to $(1 - \omega_0 F)$ is almost as good as Eq. 8, i.e.

$$\frac{K}{cD_0} = 1.0395(1 - \omega_0 F),$$

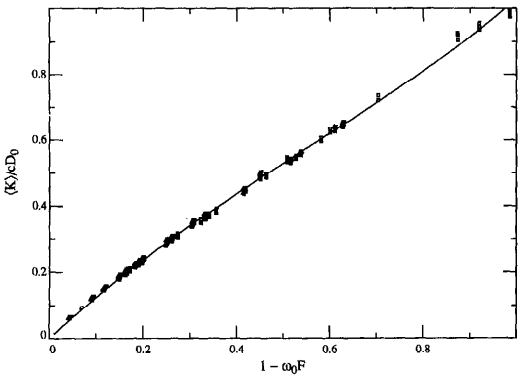

Fig. 7. As Fig. 6, but for $\langle K\rangle/cD_0$.

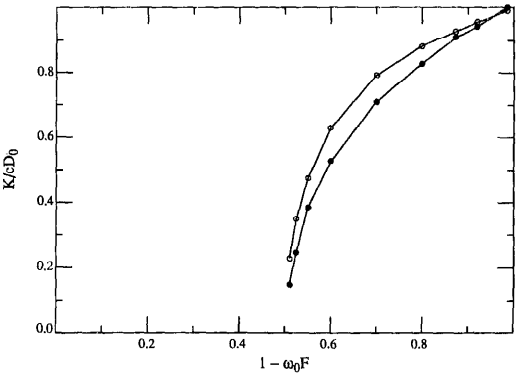

Fig. 8. K/cD_0 for a particle free ocean (Rayleigh scattering). K/cD_0—●; $\langle K\rangle/cD_0$—○.

which implies that

$$\frac{K}{D_0} = 1.0395(a + b_b), \qquad (10)$$

with an average error of 2.5%. The points on Figs. 6 and 7 with $1 - \omega_0 F > 0.85$ do not fit Eq. 8 and 9 quite as well as the rest because these points correspond to pure seawater—the phase function of which differs considerably from an ocean containing particles (*see Fig. 2*). The $K/cD_0 - (1 - \omega_0 F)$ relationship computed for an ocean free of particles is presented in Fig. 8 (for $\vartheta_0 = 0$ and no atmosphere); it differs considerably from that in Figs. 6 and 7. Since the minimum value of $(1 - \omega_w F_w)$ is 0.85 (near 400 nm), and over the range $0.85 \leq (1 - \omega_w F_w) \leq 1$ the $K/cD_0 - (1 - \omega_0 F)$ relationship for water and for the strongly forward scattering particles is very similar, the computations for the model ocean all fall very near the universal curves even though there is a large variation in the shape of the scattering phase function.

The above analysis shows that K/D_0 and $\langle K\rangle/D_0$ can be written as *explicit* algebraic functions of the inherent optical properties c, ω_0, and F (independent of the geometry of the incident light field) with an accuracy that is likely better than the accuracy with which K or $\langle K\rangle$ can be measured. Therefore we are justified in regarding the quantities K/D_0 and $\langle K\rangle/D_0$ as *inherent optical properties*. Note that if the mode of illumination of the ocean never varied, the distinction between the IOPs and the AOPs would blur (i.e. for a given set of IOPs the AOPs would always be the same at a given point in the ocean). A particular setting, wherein the (flat) sea surface is illuminated by the sun at zenith with the atmosphere absent, is unique as far as $K_d(z)$ is concerned. For a given z the value of $K_d(z)$ in this setting is a minimum over all possible modes of illumination. Thus, it is reasonable to refer to $K_d(z)$ in this situation as the *inherent* irradiance attenuation coefficient and give it the special symbol $K_d^I(z)$. Likewise, K^I and $\langle K\rangle^I$ are the inherent values of K and $\langle K\rangle$ (i.e. the values that would be measured in an imaginary ocean-atmosphere system above). The quantities K/D_0 and $\langle K\rangle/D_0$ represent excellent approximations to K^I and $\langle K\rangle^I$, i.e. the results of measurements in real situations can be transformed to this ideal setting through simple division by D_0.

To consider applying this result to a real ocean, we must examine the effect of surface roughness on this simple observation. To include surface waves in the radiative transfer code requires a statistical model of the waves. For simplicity, we assume that the surface roughness has no preferred direction (i.e. the structure of the surface is independent of wind *direction*). Then with the measurements of Cox and Munk (1954) the probability density that the sea surface at a given point has slope components z_x and z_y in the x and y directions is given approximately by

$$p(z_x, z_y) = \frac{1}{\pi\sigma^2} \exp\left(-\frac{z_x^2 + z_y^2}{\sigma^2}\right)$$

where σ^2, the slope variance, is related to the wind speed V (in m s^{-1}) through

$$\sigma^2 = 0.003 + 0.00512V.$$

The rough surface described by $p(z_x, z_y)$ is incorporated into the Monte Carlo radiative transfer code used in this work in a manner similar to that described by Plass et al. (1975). A complete examination of the effect of surface roughness on K and $\langle K\rangle$ requires a significant computational effort; however, only a few computations are required to show that the basic result above—division by D_0 renders K and $\langle K\rangle$ inherent optical properties—is still valid for an ocean with waves. A sample of the computations carried out is presented in Table 4 which provides computations of D_0, K, and $\langle K\rangle$ as a function of the surface roughness at 480 nm for $\vartheta_0 = 60°$ and $c_p/c_w = 12.3$ ($C \approx 0.5$ mg m^{-3}). Note the slow increase in D_0 with σ indicating an increasingly diffuse incident light field beneath the surface as the roughness increases. This increases K with increasing roughness; however, division of K by D_0 provides a quantity that is nearly independent of surface roughness. Interestingly, the effect of surface roughness on both $\langle K\rangle/c$ and $\langle K\rangle/cD_0$ is small (<3%) up to wind speeds of 17 m s^{-1}. These computations suggest that K/D_0 and $\langle K\rangle/D_0$ remain inherent optical properties even in the presence of surface waves; however, the value of D_0 used to form these ratios must be that which is valid in the *presence* of the rough surface.

Table 4. Computed D_0 and diffuse attenuation coefficients at 480 nm and $\vartheta_0 = 60°$ as a function of the surface roughness parameter σ.

σ	D_0	K/c	K/cD_0	$\langle K\rangle/c$	$\langle K\rangle/cD_0$
0.0	1.293	0.2624	0.2029	0.2914	0.2254
0.1	1.306	0.2632	0.2015	0.2924	0.2261
0.2	1.333	0.2733	0.2050	0.2954	0.2285
0.3	1.373	0.2833	0.2063	0.2999	0.2319

Experimental estimation of D_0

Determination of D_0 from field measurements requires the radiance distribution incident on the sea surface. This can be quantitatively determined using a camera equipped with a fisheye lens (Smith 1974; Smith et al. 1970); however, analysis of the resulting sky photographs is not simple. Earlier (Gordon 1976) I proposed a simple scheme for estimating D_0. Briefly, if $E_d(i)$ is the irradiance incident on the sea surface from source i (e.g. direct sunlight, skylight, clouds, etc.), then it is easy to show that

$$D_0 = \frac{\Sigma_i D_0(i)t(i)E_d(i)}{\Sigma_i t(i)E_d(i)}$$

where $t(i)$ is the irradiance transmittance for light from source i and $D_0(i)$ the value of D_0 that would result from source i acting alone. For a cloud-free atmosphere the only sources are the sun and the sky so this equation reduces to

$$D_0 = fD_0(\text{sun}) + (1 - f)D_0(\text{sky}) \quad (11)$$

where f is the fraction of direct sunlight in the incident irradiance transmitted through the interface, i.e.

$$f = \frac{t(\text{sun})E_d(\text{sun})}{t(\text{sun})E_d(\text{sun}) + t(\text{sky})E_d(\text{sky})}.$$

If skylight is assumed to have a uniform radiance distribution [i.e. radiance (brightness) independent of direction of viewing], Eq. 11 simplifies to

$$D_0 = \frac{f}{\cos\vartheta_{0w}} + 1.197(1 - f). \quad (12)$$

Given ϑ_0, the only unknown is f. It can be estimated by placing an irradiance meter above the surface, measuring the total incident irradiance $E_d(\text{sun}) + E_d(\text{sky})$, and then measuring the sky irradiance $E_d(\text{sky})$ by casting a shadow over the opal diffuser of the instrument.

The efficacy of Eq. 12 is tested with the Monte Carlo simulations, where $E_d(\text{sun})$ is computed from

$$E_d(\text{sun}) = \cos\vartheta_0 F_0 \times \exp[-(\tau_A + \tau_R + \tau_{Oz}) \div \cos\vartheta_0] \quad (13)$$

with F_0 the extraterrestrial solar irradiance and τ_A, τ_R, and τ_{Oz} the contributions to the optical thickness of the atmosphere from aerosol scattering, molecular (Rayleigh) scattering, and ozone absorption. $E_d(\text{sky})$ is then determined by subtraction from the

total irradiance falling on the sea surface. Even though Eq. 13 is exact, for our purposes it underestimates E_d(sun) because all photons scattered by the aerosol are assumed to be uniformly distributed over the sky; in reality a significant fraction of the aerosol scattering is through small angles and these scattered photons are still traveling in nearly the same direction as the unscattered photons. To compensate for this effect, we can obtain an upper limit on E_d(sun) by ignoring the aerosol scattering entirely, i.e. by computing E_d(sun) according to

$$E_d(\text{sun}) = \cos\vartheta_0 F_0 \times \exp[-(\tau_R + \tau_{Oz}) \div \cos\vartheta_0], \quad (14)$$

which clearly overestimates E_d(sun) since aerosol scattering does make some contribution to E_d(sky). Thus, for our purposes Eq. 13 and 14 provide lower- and upper-bound estimates of E_d(sun) and therefore of f. Comparison between D_0 computed from Eq. 12 using Eq. 13 for E_d(sun) and the "exact" values (Table 3) shows that for $0 \leq \vartheta_0 \leq 60°$ the error is $< \pm 3\%$, and for $\vartheta_0 = 80°$ Eq. 12 yields a value for D_0 that is 5–8% too low. The corresponding computations with Eq. 14 for E_d(sun) show that for $0 \leq \vartheta_0 \leq 60°$ the error is $< \mp 2\%$, and for $\vartheta_0 = 80°$ the computed value is 0.5–4% too high.

We can apply this computation to the "shadow" method suggested above for estimating f. Assume that the object used to cast the shadow of the sun is a circular disk of diameter somewhat larger than the collecting face of the irradiance meter. Then, if the disk is relatively close to the irradiance meter, a portion of the sky in the vicinity of the sun is also obscured. This would approximately correspond to estimating f with Eq. 14, i.e. photons scattered at small angles from the sun would be included in E_d(sun). Conversely, if the disk were at a great distance from the instrument only the solar disk itself would be obscured, and photons scattered at small angles from the sun become part of E_d(sky)—approximately corresponding to using Eq. 13 to estimate f. Thus we conclude that the shadow method of determining f should yield values of D_0 between the estimate obtained with Eq. 13 and 14.

In the presence of surface waves, computation of the correct value of D_0 is facilitated by the empirical observation that D_0 increases approximately in proportion to σ^2 for wind speeds up to ≈ 20 m s^{-1}. This is demonstrated in Fig. 9 for an overcast sky and for solar illumination (no atmosphere) with $\vartheta_0 = 60°$, 70°, and 80°. The dots on Fig. 9 are the computed values of D_0 and the lines are least-squares fits to $D_0 = c_1 + c_2\sigma^2$, where c_1 and c_2 are constants. The least-squares lines allow estimation of D_0 with an error of $\lesssim 2\%$. For $\vartheta_0 \leq 50°$ the variation in D_0 for $0 \leq \sigma \leq 0.3$ is $\lesssim 2\%$. Thus, for $\vartheta_0 \leq 50°$, D_0 can be computed by assuming that the sea surface is flat; for larger values of ϑ_0 (or for an overcast sky) the flat-surface values of D_0(sun) and D_0(sky) for use in Eq. 11 must be increased in accordance with Fig. 9.

Finally, in the atmospheric model used here τ_A at 550 nm was taken to be 0.25. This is very conservative, since it would correspond to a coastal atmosphere (it is typical of a continental aerosol) and is a factor of 2–3 higher than would be expected for a "clear" marine atmosphere. Therefore an estimate of f based on Eq. 14 alone (i.e. without any measurements above the surface) should provide excellent estimates of D_0 in clear marine atmospheres.

The Lambert-Beer law applied to K_d

Having established that measurements of K and $\langle K \rangle$ can be transformed into inherent optical properties in a variety of realistic situations, we now turn to the main question of this paper: the extent to which K_d satisfies the Lambert-Beer law. Consider an ocean consisting of m components, one of which is pure seawater. Let c_i^* be the specific attenuation coefficient of constituent i. Then, $c_i = c_i^* C_i$, and the total attenuation coefficient can be written

$$c = c_w + \sum_{i=1}^{m} c_i = c_w + \sum_{i=1}^{m} c_i^* C_i$$

where C_i is the *concentration* of the ith con-

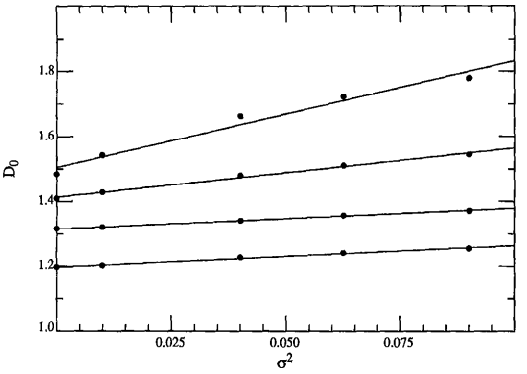

Fig. 9. D_0 as a function of σ^2. The curves from bottom to top correspond to a completely overcast sky and to solar illumination with $\vartheta_0 = 60°$, 70°, and 80°.

stituent. These relationships comprise the Lambert-Beer law, i.e. the individual attenuation coefficients are proportional to the individual concentrations and the total attenuation coefficient is a linear sum of the individual or partial attenuation coefficients. [On the surface, Eq. 5 and 6 seem to suggest that c_p is not proportional to the concentration of phytoplankton, but rather on the concentration to the 0.6 power. However, this is an artifact because c_p in the present bio-optical model includes not only the contribution of phytoplankton but also the contribution from detrital material—the relative concentration of which varies with the concentration of phytoplankton (Hobson et al. 1973). In reality the attenuation coefficient of *particles* in Case 1 waters should be written $c_p = c^*_{ph}C_{ph} + c^*_d C_d$, where the subscripts *ph* and *d* refer to phytoplankton and detritus.] Since K/D_0 and $\langle K\rangle/D_0$ are inherent optical properties, the relevant question concerns the validity of the expressions

$$\frac{K}{D_0} = \sum_{i-1}^{m} \frac{K_i}{D_0} \tag{15}$$

and

$$\frac{\langle K\rangle}{D_0} = \sum_{i=1}^{m} \frac{\langle K\rangle_i}{D_0}. \tag{16}$$

For an individual observation, the D_0s cancel from these equations; however, we will keep D_0 on both sides of these equations because Eq. 8–10 express K/D_0 and $\langle K\rangle/D_0$ as functions of the inherent optical properties and because measurements made under a variety of environmental conditions (i.e. a variety of D_0s) are often combined for statistical analysis (Baker and Smith 1982; Morel 1988).

Clearly, if Eq. 10 is used for K/D_0, its linear dependence on the inherent optical properties means that the error in Eq. 15 is no more than the error in Eq. 10, i.e.

$$\begin{aligned}\frac{K}{D_0} &= 1.0395(a + b_b)\\ &= 1.0395\left[\sum_{i=1}^{m} a_i + \sum_{i=1}^{m} (b_b)_i\right]\\ &= \sum_{i=1}^{m} 1.0395[a_i + (b_b)_i]\\ &= \sum_{i=1}^{m} \frac{K_i}{D_0}.\end{aligned}$$

Thus, any error in the Lambert-Beer law *over and above* the error due to the fact that division of K and $\langle K\rangle$ by D_0 does not remove all of the geometric effects, i.e. the scatter of the points about the smooth curve in Figs. 6 and 7 is due to *nonlinearities* in the dependence of K and $\langle K\rangle/D_0$ on the inherent optical properties. To understand the magnitude of this nonlinear contribution to the error we consider a hypothetical model. Assume that Eq. 9 for $\langle K\rangle/cD_0$—the more nonlinear of the two relationships—is exact and that the ocean consists only of water and plankton. We use ω_w and ω_p from Table 2 with $F_w = 0.50$. Particle phase functions C, M, and T have $F_p = 0.9819$, 0.9856, and 0.9880, so F_p is chosen to be 0.985. The relative concentration of particles, as measured by c_p/c, is then varied from 0 to 1. The true value of $\langle K\rangle/D_0$, $\langle K\rangle_T/D_0$, is computed from Eq. 9 using the value of $\omega_0 F$ for the mixture, i.e. with

$$\omega_0 F = \frac{\omega_p F_p c_p + \omega_w F_w c_w}{c_p + c_w}.$$

The Lambert-Beer law value, $\langle K\rangle_B/D_0$, is computed from

$$\frac{\langle K\rangle_B}{D_0} = \frac{\langle K\rangle_w}{D_0} + \frac{\langle K\rangle_p}{D_0}$$

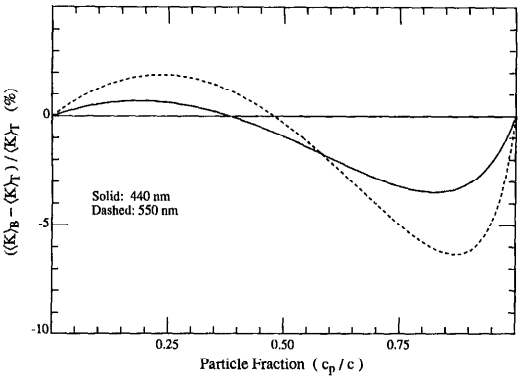

Fig. 10. Relative error (%) in $\langle K\rangle_B$ as a function of the relative concentration of particles.

with $\langle K\rangle_w/D_0$ and $\langle K\rangle_p/D_0$ individually determined by Eq. 9 using $\omega_w F_w$ and $\omega_p F_p$, respectively. This procedure can be visualized graphically by considering Fig. 7. The value of $\langle K\rangle_B/cD_0$ falls on a *straight line* between two points on the least-squares curve located at $\omega_0 F = \omega_w F_w$ and $\omega_0 F = \omega_p F_p$, while $\langle K\rangle_T/cD_0$ is on the curve itself. The relative error in $\langle K\rangle_B/D_0$ is then computed by means of

$$\frac{\langle K\rangle_B - \langle K\rangle_T}{\langle K\rangle_T}.$$

This error is shown in Fig. 10 as a function of (c_p/c). We see that the *maximum* error at 440 nm is $\approx$3%, and the maximum error at 550 nm is $\approx$6%. Had $\omega_p(440) = 0.80$ been used in this example the error at 440 nm would have been <2%. Since $\omega_p(440) = 0.86$ is near the upper limit for phytoplankton [e.g. Bricaud et al. 1983 measured $\omega_p(440) = 0.88$ for the coccolithophore *Emiliana huxleyi* which is known to be a very strong scatterer], it is believed that the error at 440 nm will typically be <3% and often <2%. With Eq. 7, c_p/c can be related to the pigment concentration for this two-component example. The maximum error in the Lambert-Beer law at 440 nm occurs when $C \approx 0.09$ mg m^{-3}, while at 550 nm it occurs when $C \approx 1.70$ mg m^{-3}. These errors are to a certain extent dependent on the use of Eq. 9. Had a different fit to the simulations been used, e.g. a higher order polynomial in $(1 - \omega_0 F)$ to better fit the computed $\langle K\rangle/D_0$ near $1 - \omega_0 F = 1$, a different error distribution with c_p/c would result. To assess the true error the reader should sketch what he or she believes to be the "best" smooth curve (or segmented curve) through the points in Fig. 7 and then use the graphical method above to assess the error in the Lambert-Beer law, including the scatter of the points about the "best" line. When I do this for the model values of ω_p, F_p, ω_w, and F_w, I find the *maximum* error to be about 5% for 440 nm and about 10% for 550 nm for Case 1 waters.

The optical model developed for this work is strictly applicable to Case 1 waters only; however, it is of interest to consider the possible extension of these results to Case 2 waters (i.e. Case 1 waters subjected to high concentration of suspended sediment and/or absorbing yellow substances). The basic relationships between K/D_0 and $\langle K\rangle/D_0$ and the IOPs provided in Figs. 6 and 7 are expected to be valid in Case 2 waters since one of the particle phase functions used in the simulations was measured in Case 2 waters and additional values of ω_p (0.50, 0.70, and 0.99) over and above those in Table 2 were used in the computations and have been included in the analysis.

The Case 1 example concerned adding strong scatterers (plankton and their detritus) to a strongly absorbing medium (seawater). If very weak scatterers ($\omega_p \ll 1$), or nonscatterers such as yellow substances ($\omega_p = 0$), are added to pure seawater, the error in the Lambert-Beer law can be assessed by examination of the region of Fig. 7 near $1 - \omega_0 F = 1$. Since water has $\omega_0 \lesssim 0.30$, the error in the Lambert-Beer law is essentially the error in the "best" fit to the simulations in this region, i.e. about $\pm$2%. If particles that scatter more weakly than phytoplankton, i.e. $\omega_p \lesssim 0.8$, are added to water, the Lambert-Beer law should be even better satisfied than for Case 1 waters at 440 nm. Only the extreme case of adding nonabsorbing particles $\omega_p = 1$ to pure seawater remains to be considered. For this the Lambert-Beer law always predicts a $\langle K\rangle$ value that is too small, and the error can become excessive (~30%) in the region $1 - \omega_0 F \lesssim$

0.3. In fact, the error is $\lesssim$20% when $\omega_0 F \leq$ 0.8 at 440 nm and when $\omega_0 F \leq 0.7$ at 550 nm. Thus, the Lambert-Beer law will fail in Case 2 waters dominated by high concentrations of nonabsorbing suspended materials; however, if high concentrations of yellow substances occur simultaneously with the nonabsorbing particles, $\omega_0 F$ for the mixture may be sufficiently low so the error in the Lambert-Beer law is not excessive. Unfortunately, the Lambert-Beer law will also fail in certain coccolithophore blooms in Case 1 waters as well. For example, the optical properties of blooms of *E. huxleyi* have been observed (Holligan et al. 1983) to be dominated at times by nonabsorbing detached coccoliths ($\omega_p = 1$). The same difficulties with the Lambert-Beer law that occur in sediment-dominated Case 2 waters will also apply to such blooms even though they satisfy the definition of Case 1 waters, i.e. the optical properties are determined by water and by phytoplankton and their immediate detrital material.

It is important to understand that the near-validity of the Lambert-Beer law rests squarely on the near-linearity of the relationships shown in Figs. 6 and 7, i.e. that the quantities involved must be inherent optical properties is a necessary but not sufficient condition for the validity of the law. For example, if all particles in Case 1 waters were sufficiently small to scatter light with the same phase function as pure seawater, the dependence of K/cD_0 and $\langle K\rangle/cD_0$ on $1 - \omega_0 F$ would be given by Fig. 8. In such a case, if phytoplankton and detritus were mixed with water at 550 nm, the Lambert-Beer law value of K for the resulting mixture would fall along a straight line from $1 - \omega_0 F \approx 0.54$ to $1 - \omega_0 F \approx 1$, while the actual K values would fall along the curve. Clearly, very large departures from Lambert-Beer law would be seen for all values of c_p/c in such an ocean. Thus, the near-validity of the Lambert-Beer law in the case of a realistic ocean is seen to result from the interplay of three *independent* facts: the dependence of the diffuse attenuation coefficients on the geometric structure of the light field can be removed (division by D_0); pure seawater is a much better absorber than scatterer at optical frequencies ($1 - F_w\omega_w \gtrsim 0.85$); and the phase functions for particles suspended in the ocean differs significantly from that of pure seawater (Fig. 1).

Finally it is of interest to determine the accuracy with which one can estimate the diffuse attenuation coefficient of an ocean consisting solely of pure seawater through extrapolation of K_d values measured in a real ocean to the limit of zero particle concentration. As mentioned earlier, this is the scheme that Smith and Baker and others have used to estimate K_d for pure water (Baker and Smith 1982; Smith and Baker 1978*a*,*b*, 1981). For this purpose we have computed $\langle K\rangle$ as a function of c at 480 nm by letting C in Eq. 13 range from 0 to 4.5 mg m^{-3}. Figure 11 shows the results for $\vartheta_0 = 0°$, 60°, and for overcast skies. The lines on the graph correspond to linear least-squares fits to the computed points with $C > 0$ ($c_p > 0$ or $c > c_w$), i.e. the point on each line corresponding to pure water was left out of the fit. The least-squares line was then extrapolated to $c_p = 0$ to determine $\langle K\rangle$ in the absence of particles, which corresponds to extrapolating C to zero pigment concentration. As seen from the figure, the extrapolated line falls very close to the computed values of $\langle K\rangle$ for pure seawater. In fact, the difference between the computed and extrapolated values of $\langle K\rangle_w$ are, respectively, 3.8, 1.9, and 1.5%. In this example, the incident illumination is the same for each value of c along the individual least-squares lines, and the linearity of the $\langle K\rangle - c$ relationship again verifies that the Lambert-Beer law is valid for $\langle K\rangle$ in Case 1 waters when the mode of illumination is held fixed.

In practice it would be impossible to arrange this experimentally. In the field, each data point would likely correspond to a different incident light field. However, we have seen that dividing $\langle K\rangle$ by D_0 removes most of the effects of the geometric structure of the light field. To assess the efficacy of determining $\langle K\rangle_w$ from extrapolation to $c_p = 0$ in more realistic situations, I applied the above extrapolation procedure to $\langle K\rangle/D_0$ obtained from *all* of the simulations (i.e. all illumination conditions were treated equally and included in the analysis). Figure 12

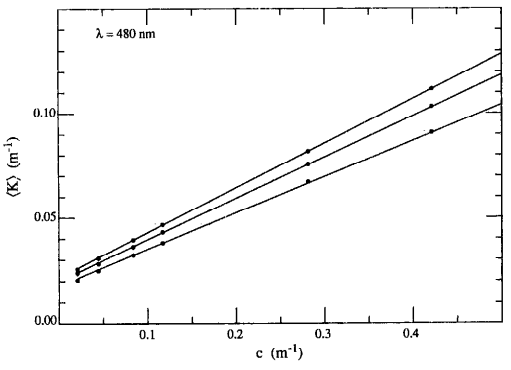

Fig. 11. $\langle K \rangle$ at 480 nm as a function of c for particle phase function M. The lower and upper lines are for $\vartheta_0 = 0°$ and 60°, and the center line is for an overcast sky.

shows the results of the extrapolation at 480 nm, and Table 5 compares the extrapolated value of $\langle K \rangle_w / D_0$ with the inherent value of $\langle K \rangle_w$ (i.e. $\langle K \rangle_w^I$), the value of $\langle K \rangle$ for an ocean composed of pure seawater computed with the atmosphere removed and with the sun at zenith. Table 5 suggests that the extrapolation procedure can yield $\langle K \rangle_w^I$ to within ~2%. Note, however, that Fig. 12 shows that large errors in $\langle K \rangle_w^I$ are possible if it is determined from a small amount of data with $c_p \gg c_w$. For example, if the highest value of $\langle K \rangle / D_0$ at $c \approx 0.27$ m^{-1} and the lowest value at $c \approx 0.42$ m^{-1} were used, the extrapolated value of $\langle K \rangle_w / D_0$ would be ≈ 0.038 m^{-1}—an error of nearly a factor of 2. Thus, as we would expect, the experimental determination of $\langle K \rangle_w^I$ must be carried out by excluding turbid waters from the analysis.

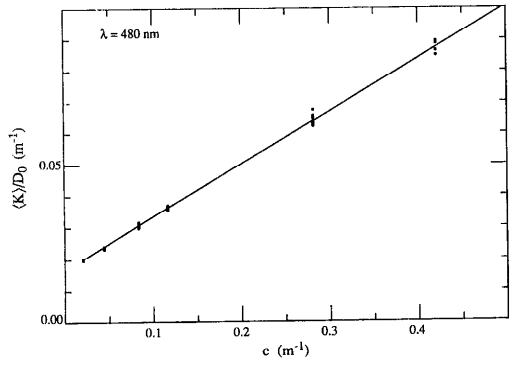

Fig. 12. $\langle K \rangle / D_0$ as a function c at 480 nm. The points are Monte Carlo simulations for various values of ϑ_0; the line is a least-squares fit to the points with $c_p > c_w$.

Table 5. The inherent $\langle K \rangle_w^I$ and the extrapolated value of $\langle K \rangle_w / D_0$ in m^{-1} for the three wavelengths.

	440 nm	480 nm	550 nm
$\langle K \rangle_w^I$	0.0182	0.0202	0.0652
$\langle K \rangle_w / D_0$	0.0178	0.0202	0.0667

From the extrapolated values of K_w and $\langle K \rangle_w$, it is natural to try to estimate a_w. In fact, the values of a_w used here were computed by Smith and Baker (1981) from their estimated values of K_w using

$$K_w = a_w + (b_b)_w = a_w + 0.5 b_w$$

where $(b_b)_w$ is the backscattering coefficient of pure seawater, along with Morel's laboratory measurements of b_w (Morel 1974). However, Fig. 8 shows that, for $\omega_0 F$ near 1, better approximations are

$$K_w^I = a_w + 0.62 b_w$$

and

$$\langle K \rangle_w^I = a_w + 0.72 b_w,$$

leading to values of a_w that are slightly lower than Smith and Baker's in the spectral region below 550 nm. By looking at the variation of K_d with a and b in the asymptotic light field for isotropic scattering, Bohren (1984) suggested that the Smith and Baker a_w values were too low and proposed larger values based on using $K_w = a_w + b_w$. My computations here support Bohren's contention; however, the true correction is less than half as large at the surface as he proposed.

My conclusions concerning the validity of the Lambert-Beer law are in conflict with those of Stavn (1988). He suggested that there is a systematic error in the Lambert-Beer law and that this error can lead to large errors in partitioning absorption between water and plankton. Briefly, Stavn based his objections on the exact relationship

$$K_d = \frac{a}{\bar{\mu}} (1 - R) + R K_u$$

where $R = E_u / E_d$ and $K_u = -(1/E_u)\, dE_u /$

dz, which can be derived in a straightforward manner from Gershun's law and is valid for all z. If $R \ll 1$ and $K_u \approx K_d$, which are usually excellent approximations in Case 1 waters or yellow substance-dominated Case 2 waters, then $K_d \approx a/\bar{\mu}$. The identity $a = a_w + a_p$ can be rewritten

$$\frac{a}{\bar{\mu}} = \frac{a_w}{\bar{\mu}} + \frac{a_p}{\bar{\mu}}$$
$$= \left(\frac{\bar{\mu}_w}{\bar{\mu}}\right)\frac{a_w}{\bar{\mu}_w} + \left(\frac{\bar{\mu}_p}{\bar{\mu}}\right)\frac{a_p}{\bar{\mu}_p}$$

where $\bar{\mu}_w$ and $\bar{\mu}_p$ are the values of $\bar{\mu}$ in an ocean with the same radiance distribution incident on the sea surface and the same surface roughness, but for which $c_p = 0$ and $c_w = 0$, respectively. Note that the values of $\bar{\mu}_w$ and $\bar{\mu}_p$ at a given depth are fixed (i.e. they *do not* depend on c_p/c_w). Using $K_d \approx a/\bar{\mu}$, $K_w \approx a_w/\bar{\mu}_w$, etc., we have

$$K_d(z) \approx \left[\frac{\bar{\mu}_w(z)}{\bar{\mu}(z)}\right] K_w(z) + \left[\frac{\bar{\mu}_p(z)}{\bar{\mu}(z)}\right] K_p(z).$$

This equation shows that the Lambert-Beer law applied to $K_d(z)$ is approximately valid only when $\bar{\mu}(z) \approx \bar{\mu}_w(z) \approx \bar{\mu}_p(z)$, which occurs near the surface where the value of $\bar{\mu}$ is determined mostly by the radiance distribution incident on the sea surface and on surface roughness. In fact, near the surface $\bar{\mu}(z) \approx \bar{\mu}_w(z) \approx \bar{\mu}_p(z) \approx 1/D_0$. As we move deeper into the water column, $\bar{\mu}$ deviates systematically from $\bar{\mu}_w$ and $\bar{\mu}_p$ with $\bar{\mu}_p(z) < \bar{\mu}(z) < \bar{\mu}_w(z)$. On this basis, we expect that the Lambert-Beer law should work reasonably well near the surface but should lead to systematic errors as depth is increased.

The present paper quantitatively assesses these errors, showing that the law applied to K and $\langle K\rangle$ works well for $z \lesssim z_{10}$. Stavn on the other hand suggested that large errors are possible even near $z = 0$. His analysis, however, was based on the Smith and Baker (1981) estimations of K_w and a_w, which we have seen are inconsistent with one another. Stavn also assumed that K_w is independent of the distribution of radiance incident on the sea surface and independent of depth. When the revised values of a_w determined from K_w^I are used along with the actual values of K_w near the surface ($K_w = D_0 K_w^I$) and the small increase of K_w^I with depth is considered, the errors on which Stavn based his objection to the Lambert-Beer law vanish (within his error limits) in the upper 20 m of the water column in three of the four cases he examined. Note that this occurs even without considering the rather large uncertainties Smith and Baker give for their estimated K_w values. Below this surface layer, it appears that Stavn's conclusion becomes valid, i.e. the Lambert-Beer law may lead to significant systematic errors when applied to $K_d(z)$ at a given depth z for $z \gtrsim z_{10}$. Determination of these errors, a question which is very important for the interpretation of measurements from moorings, will require further study both through measurement with modern instrumentation and through simulation. Only the application of the Lambert-Beer law to K and $\langle K\rangle$ has been addressed here.

Concluding remarks

By simulating the transport of radiation in a realistic ocean-atmosphere system and treating the results as experimental data obtained under carefully controlled conditions, it has been shown that K and $\langle K\rangle$, when modified through division by D_0 are, to a high degree of accuracy, inherent optical properties. A simple scheme for estimating D_0 for individual experimental situations is provided. Furthermore it is shown that for Case 1 waters K/D_0 and $\langle K\rangle/D_0$ satisfy the Lambert-Beer law to a reasonable degree of accuracy (maximum error $\approx$5–10%, depending on wavelength). The errors are not significantly increased for Case 2 waters as long as waters for which the IOPs are dominated by nonabsorbing suspended particles are avoided. The near-validity of the Lambert-Beer law in this situation, where there are compelling reasons to believe that it should fail, is traced to three *independent* facts: the dependence of the diffuse attenuation coefficients on the geometric structure of the light field can be removed; pure seawater is a much better absorber than

scatterer at optical frequencies; and the phase functions for particles suspended in the ocean differs significantly from those of pure seawater. If any of these facts were false the Lambert-Beer law would fail. Finally, it is shown that extrapolation of K/D_0 and $\langle K\rangle/D_0$ to the limit $c \to c_w$ yields quantities that are within 2% of K_w^I and $\langle K\rangle_w^I$, i.e. the value of K and $\langle K\rangle$ that would be measured for an ocean consisting of pure seawater with the sun at zenith and the atmosphere removed.

When D_0 is left out of the analysis, the result is a rather large additional error in the Lambert-Beer law (e.g. *see* Figs. 4 and 5). However, Table 3 shows that when measurements are restricted to situations where $0 \leq \vartheta_0 \leq 40°$ the total variation in D_0 is only from 1 to about 1.16, a ±8% variation around 1.08. An analysis of $\langle K\rangle$ so restricted shows that in Case 1 waters the error doubles over that when D_0 is included. Thus, when measurements are restricted to clear skies near noon, the Lambert-Beer law applied to $\langle K\rangle$ itself should be in error by no more than 10–20%. This may account for the success of the law for in situ observation and analysis of phytoplankton absorption (i.e. investigators may have restricted the analysis to data taken under "ideal" conditions similar to these).

The analysis of oceanic properties with K_d is useful because of the relative simplicity of the instrumentation required for its measurement. The near-validity of the Lambert-Beer law for all but the most strongly scattering of natural waters allows the partial diffuse attenuation coefficients, in the sense of Eq. 1, 15, and 16, to be determined. Since the partial, as well as the total, K_d functions (K and $\langle K\rangle$) are in the first approximation proportional to $a + b_b$ for those species for which $a \gg b_b$ (e.g. phytoplankton and dissolved organic material), measurement of K or $\langle K\rangle$ provides a direct estimate of a from K_i/D_0 or $\langle K\rangle_i/D_0$. Thus, until the development of an in situ spectral absorption meter, measurement of K_d appears to be the only available in situ means of estimating $a(\lambda)$. Note, however, that in general the medium will contain more than two components (e.g. water, plankton and detritus, yellow substances, etc.) and separation of the components can only be carried out in a statistical sense.

Application of these results to field experiments presents several difficulties. The first stems from the fact that K/D_0, which satisfies the Lambert-Beer law better than $\langle K\rangle/D_0$, is very difficult to measure in practice due to the strongly fluctuating irradiance at the surface resulting from the presence of surface capillary waves and the difficulty of accurately determining the depth of the instrument near the surface due to the presence of surface gravity waves. Thus, measurement of $\langle K\rangle/D_0$, which is significantly less influenced by the surface effects, is preferred from an experimental point of view; however, in the case of oceanic water, the mixed layer must be sufficiently deep so that $z_{10} = \tau_{10}/c$ is within the mixed layer and the water can be treated as homogeneous. For the limiting case of an ocean free of particles, this would require a mixed layer of ≈125, 115, and 35 m at 440, 480, and 550 nm. A second difficulty concerns the determination of D_0 in the presence of broken clouds. In this case Eq. 12 will not apply and the only viable method is to photograph the sky with a fisheye lens. Finally, the presence of whitecaps on the sea surface will further modify the internal geometry of the light field and influence D_0. Their effect cannot be discussed further without knowledge of their optical properties.

References

AUSTIN, R. W., AND T. J. PETZOLD. 1981. Remote sensing of the diffuse attenuation coefficient of sea water using the Coastal Zone Color Scanner, p. 239–256. *In* J. R. F. Gower [ed.], Oceanography from space. Plenum.

BAKER, K. S., AND R. C. SMITH. 1979. Quasi-inherent characteristics of the diffuse attenuation coefficient for irradiance, p. 60–63. *In* Ocean Optics 6, Proc. SPIE **208.**

———, AND ———. 1982. Bio-optical classification and model of natural waters. 2. Limnol. Oceanogr. **27:** 500–509.

BOHREN, C. F. 1984. Absorption of pure water: New upper bounds between 400 and 580 nm. Appl. Opt. **23:** 2868.

BRICAUD, A., A. MOREL, AND L. PRIEUR. 1983. Optical efficiency factors of some phytoplankters. Limnol. Oceanogr. **28:** 816–832.

CASE, K. M. 1957. Transfer problems and the reciprocity principle. Rev. Mod. Phys. **29:** 651–663.

COX, C., AND W. MUNK. 1954. Measurements of the roughness of the sea surface from photographs of the sun's glitter. J. Opt. Soc. Am. **44:** 838–850.

DEIRMENDJIAN, D. 1969. Electromagnetic scattering on spherical polydispersions. Elsevier.

ELTERMAN, L. 1968. UV, visible, and IR attenuation for altitudes to 50 km. AFCRL Rep. 68-0153. AFCRL, Bedford, Mass.

GERSHUN, A. 1939. The light field. J. Math. Phys. **18:** 51–151.

GORDON, H. R. 1976. Radiative transfer in the ocean: A method for determination of absorption and scattering properties. Appl. Opt. **15:** 2611–2613.

———. 1979. The diffuse reflectance of the ocean: The theory of its augmentation by chlorophyll *a* fluorescence at 685 nm. Appl. Opt. **18:** 1161–1166.

———. 1980. Irradiance attenuation coefficient in a stratified ocean: A local property of the medium. Appl. Opt. **19:** 2092–2094.

———. 1982. Interpretation of airborne oceanic Lidar: Effects of multiple scattering. Appl. Opt. **21:** 2996–3001.

———. 1987. A bio-optical model describing the distribution of irradiance at the sea surface resulting from a point source embedded in the ocean. Appl. Opt. **26:** 4133–4148.

———, O. B. BROWN, AND M. M. JACOBS. 1975. Computed relationships between the inherent and apparent optical properties of a flat homogeneous ocean. Appl. Opt. **14:** 417–427.

———, AND A. Y. MOREL. 1983. Remote assessment of ocean color for interpretation of satellite visible imagery: A review. Springer.

HOBSON, L. A., D. W. MENZEL, AND R. T. BARBER. 1973. Primary productivity and the sizes of pools of organic carbon in the mixed layer of the ocean. Mar. Biol. **19:** 298–306.

HOLLIGAN, P. M., M. VIOLLIER, D. S. HARBOUR, P. CAMUS, AND M. CHAMPAGNE-PHILIPPE. 1983. Satellite and ship studies of coccolithophore production along the continental shelf edge. Nature **304:** 339–342.

KIRK, J. T. O. 1981. Monte Carlo study of the nature of the underwater light field in, and the relationships between optical properties of, turbid yellow waters. Aust. J. Mar. Freshwater Res. **32:** 517–532.

———. 1983. Light and photosynthesis in aquatic ecosystems. Cambridge.

———. 1984. Dependence of relationship between inherent and apparent optical properties of water on solar altitude. Limnol. Oceanogr. **29:** 350–356.

MOREL, A. 1974. Optical properties of pure water and pure sea water, p. 1–24. *In* N. G. Jerlov and E. Steemann Nielsen [eds.], Optical aspects of oceanography. Academic.

———. 1980. In-water and remote measurement of ocean color. Boundary-Layer Meteorol. **18:** 177–201.

———. 1988. Optical modeling of the upper ocean in relation to its biogenous matter content (Case I waters). J. Geophys. Res. **93:** 10,749–10,768.

———, AND A. BRICAUD. 1981. Theoretical results concerning light absorption in a discrete medium, and application to specific absorption of phytoplankton. Deep-Sea Res. **28:** 1375–1393.

———, AND L. PRIEUR. 1977. Analysis of variations in ocean color. Limnol. Oceanogr. **22:** 709–722.

———, AND R. C. SMITH. 1982. Terminology and units in optical oceanography. Mar. Geod. **5:** 335–349.

PETZOLD, T. J. 1972. Volume scattering functions for selected natural waters. Scripps Inst. Oceanogr. Visibility Lab. SIO Ref. 72-78.

PLASS, G. N., G. W. KATTAWAR, AND J. A. GUINN. 1975. Radiative transfer in the earth's atmosphere: Influence of ocean waves. Appl. Opt. **14:** 1924–1936.

PREISENDORFER, R. W. 1959. Theoretical proof of the existence of characteristic diffuse light in natural waters. J. Mar. Res. **18:** 1–9.

———. 1961. Application of radiative transfer theory to light measurements in the sea. Int. Union Geod. Geophys. Monogr. 10, p. 11–30.

———. 1976. Hydrologic optics. V. 1. NTIS PB 259793/8ST. Natl. Tech. Inform. Serv., Springfield, Va.

PRIEUR, L., AND S. SATHYENDRANATH. 1981. An optical classification of coastal and oceanic waters based on the specific absorption curves of phytoplankton pigments, dissolved organic matter, and other particulate materials. Limnol. Oceanogr. **26:** 671–689.

SATHYENDRANATH, S. 1981. Influence des substances en solution et en suspension dans les eaux de mer sur l'absorption er la reflectance. Modelisation et applications a'la teledetection. Ph.D. thesis, 3rd cycle, Univ. Pierre et Marie Curie, Paris. 123 p.

SMITH, R. C. 1974. Structure of solar radiation in the upper layers of the sea, p. 95–119. *In* N. G. Jerlov and E. Steemann Nielsen [eds.], Optical aspects of oceanography. Academic.

———, R. W. AUSTIN, AND J. E. TYLER. 1970. An oceanographic radiance distribution camera system. Appl. Opt. **9:** 2015–2022.

———, AND K. S. BAKER. 1978*a*. The bio-optical state of ocean waters and remote sensing. Limnol. Oceanogr. **23:** 247–259.

———, AND ———. 1978*b*. Optical classification of natural waters. Limnol. Oceanogr. **23:** 260–267.

———, AND ———. 1981. Optical properties of the clearest natural waters (200–800 nm). Appl. Opt. **20:** 177–184.

STAVN, R. H. 1988. Lambert-Beer law in ocean waters: Optical properties of water and of dissolved/suspended material, optical energy budgets. Appl. Opt. **27:** 222–231.

———, AND A. D. WEIDEMANN. 1988. Optical modeling of clear ocean light fields: Raman scattering effects. Appl. Opt. **27:** 4002–4011.